electronics

*Article*

# Optimal Pole-Swapping in Bipolar DC Networks Using Discrete Metaheuristic Optimizers

**Oscar Danilo Montoya [1,2,*], Ángeles Medina-Quesada [3] and Jesus C. Hernández [3,*]**

[1] Grupo de Compatibilidad e Interferencia Electromagnética, Facultad de Ingeniería, Universidad Distrital Francisco José de Caldas, Bogotá 110231, Colombia
[2] Laboratorio Inteligente de Energía, Facultad de Ingeniería, Universidad Tecnológica de Bolívar, Cartagena 131001, Colombia
[3] Department of Electrical Engineering, University of Jaén, Campus Lagunillas s/n, Edificio A3, 23071 Jaén, Spain; aquesada@ujaen.es
* Correspondence: odmontoyag@udistrital.edu.co (O.D.M.); jcasa@ujaen.es (J.C.H.)

**Abstract:** Bipolar direct current (DC) networks are emerging electrical systems used to improve the distribution capabilities of monopolar DC networks. These grids work with positive, negative, and neutral poles, and they can transport two times the power when compared to monopolar DC grids. The distinctive features of bipolar DC grids include the ability to deal with bipolar loads (loads connected between the positive and negative poles) and with unbalanced load conditions, given that the loads connected to the positive and neutral poles are not necessarily equal to the negative and neutral ones. This load imbalance deteriorates voltages when compared to positive and negative poles, and it causes additional power losses in comparison with balanced operation scenarios. This research addresses the problem of pole-swapping in bipolar DC networks using combinatorial optimization methods in order to reduce the total grid power losses and improve the voltage profiles. Bipolar DC networks with a non-solidly grounded neutral wire composed of 21 and 85 nodes are considered in the numerical validations. The implemented combinatorial methods are the Chu and Beasley genetic algorithm, the sine-cosine algorithm, and the black-hole optimization algorithm. Numerical results in both test feeders demonstrate the positive effect of optimal pole-swapping in the total final power losses and the grid voltage profiles. All simulations were run in the MATLAB programming environment using the triangular-based power flow method, which is intended for radial distribution system configurations.

**Keywords:** bipolar DC networks; optimal pole-swapping problem; unbalanced distribution networks; monopolar constant power terminals; triangular-based power flow formulation; operation with neutral floating

check for updates

**Citation:** Montoya, O.D.; Medina-Quesada, Á.; Hernández, J.C. Optimal Pole-Swapping in Bipolar DC Networks Using Discrete Metaheuristic Optimizers. *Electronics* **2022**, *11*, 2034. https://doi.org/10.3390/electronics11132034

Academic Editor: Nikolaos M. Manousakis

Received: 8 June 2022
Accepted: 27 June 2022
Published: 29 June 2022



## 1. Introduction

Bipolar DC distribution has attracted the attention of both academia and the industry due to its advantages over traditional AC distribution networks and monopolar DC configurations [1,2]. In comparison with AC networks, bipolar DC networks do not require reactive power and frequency control, which makes them easy to control, since the control variable is only the magnitude of the voltage at each pole (positive and negative) in the feeding bus [3]. With respect to monopolar DC networks, bipolar DC networks can transport two times the power, and they allow interconnecting loads between the positive and negative poles (i.e., two-pole loads) for special applications [4,5].

Even though bipolar DC networks are efficient when compared to monopolar DC configurations or easily manageable in comparison with AC conventional systems, their analysis requires specialized tools regarding control and optimization [6]. In the case of control, efficient nonlinear control methods are required to support constant voltages in the substation while considering the neutral wire and the positive and negative poles and ensuring stability during closed-loop operation for constant power terminals [7]. The main challenge with respect to control is dealing with the negative resistance effect of the constant power terminals in converters for AC/DC applications [8]. The optimization area is not the exception, since efficient power flow tools, optimal power flow methods, and so on are required to optimize the grid performance regarding power loss minimization or voltage profile improvements [2], among other applications. This research focuses on the optimization of bipolar DC configurations in order to deal with power loss minimization. These power losses are mainly caused by imbalances in the monopolar loads (i.e., differences between total positive-to-neutral and negative-to-neutral loads) [9].

In the current literature, the analysis of bipolar DC networks is still a young field of research, and there are few works that concentrate on it. Ref. [9] proposed a derivative-free power flow approach to deal with voltage calculation in bipolar DC networks while considering load imbalances and the possibility of working with solidly grounded or floating neutral wire. Numerical results in the 21-bus grid and the 85-bus grid showed the effectiveness of this power flow method regarding processing times, the number of iterations, and convergence. Ref. [10] solved the power flow problem for bipolar DC networks by considering constant power terminals. A 3-bus system was used for validating the power flow model. This model was developed using the nodal voltage method. However, the authors do not propose any innovative solution alternative, and they just implemented the electrical circuit in the PSCAD/EMTDC software.

Regarding the optimal power flow solution, multiple methodologies have been proposed in the current literature. Ref. [2] addressed the optimal power flow problem for bipolar DC networks with multiple monopolar and bipolar constant power terminals, with the main advantage that the neutral cable is considered in their formulation. The goal of this paper is to calculate the locational marginal prices of all the nodes in the network. To this effect, the authors relax the hyperbolic relations between voltages and power using linearization methods. This relaxation simplifies the complication of the power flow problem and allows turning it into a linear or quadratic programming model with linear constraints. In [11], an optimal power flow approach for bipolar DC networks is proposed which involves the classical current injection method using the Newton–Raphson representation. The aim of this research is to minimize the grid voltage imbalances caused by monopolar constant power loads. A quadratic programming model with linear constraints based on the Jacobian matrix is used to solve optimal power flow problems by means of a recursive sequential evaluation. Even though this proposed approach is novel, the authors do not present validations with combinatorial or nonlinear programming methods.

As for optimal pole swapping applications, Ref. [12] proposed a multi-objective optimization model to redistribute pole-to-neutral loads between positive and negative poles. Nevertheless, they did not consider the hyperbolic relations between voltage and power, and they only worked with resistive loads. This simplification allows obtaining a mixed-integer linear programming model.

Based on the aforementioned state-of-the-art review, it was possible to identify that only [12] presented a solution methodology for dealing with the optimal pole-swapping problem in bipolar DC grids. However, the model was simplified and does not consider the effect of constant power terminals in its formulation. This allowed identifying a research opportunity regarding the solution of the optimal pole-swapping problem in bipolar DC grids while considering multiple monopolar constant power loads through a master–slave optimization approach. In the master stage, three different metaheuristic optimization methodologies are employed to define the load connection at each node from positive-to-neutral and negative-to-neutral poles. To decide on the connection of these loads to each node a binary codification is implemented, where 0 implies maintaining the initial load connection and 1 means interchanging monopolar loads between poles. The selected metaheuristic techniques selected are (i) the Chu and Beasley genetic algorithm (CBGA), (ii) the sine-cosine algorithm (SCA), and (iii) the black-hole optimizer (BHO). In the slave stage, the triangular-based power flow formulation proposed in [9] is employed to evaluate the total grid power losses for each possible set of load connections provided by the master stage.

Note that the selection of the three metaheuristic optimizers was made based on the fact that they are different in nature. The CBGA, for instance, was inspired by Darwin's evolution theory, i.e., it is a nature-inspired optimizer; the SCA corresponds to a combinatorial optimization method that is mathematically inspired by the circular behavior of the sine and cosine trigonometric functions, and the BHO approach is a combinatorial optimization method from the family of physical-inspired algorithms. These selections were made to verify whether the theory that inspired each optimizer influences the final solution of the studied optimization problem. It is worth mentioning that all of these optimizers are population-based algorithms, and their differences lie in the mathematical structure of the evolution rules.

Numerical results in the 21- and 85-bus grids confirm that all the three metaheuristic optimizers find adequate power loss reductions compared to the benchmark cases with reduced processing times. In the 21-bus grids, the reductions with respect to the benchmark case were 3.94%, and the processing times were lower than 9 s; whereas, for the 85-bus system, the power loss reductions were lower than 10.17% and the average processing times were lower than 134 s.

The remainder of this research is structured as follows: Section 2 presents the exact mixed-integer nonlinear programming model that represents the optimal pole-swapping problem in bipolar DC networks with multiple monopolar and bipolar constant power terminals; Section 3 describes the main aspects of each of the proposed metaheuristic optimizers, i.e., codification, initial population, and evolution rules, among others, and it presents the general power flow formula based on the upper triangular matrix representation; Section 4 describes the main characteristics of the test feeders, which are composed of 21 and 85 buses with radial structures; Section 5 presents the numerical validation of the proposed master–slave optimizers, as well as their analysis, comparisons, and discussions; finally, Section 8 shows the main concluding remarks obtained from this research, as well as some proposals for future work.

## 2. Formulation of the Power Flow Problem

To represent the problem regarding optimal pole-swapping in bipolar DC networks while considering the neutral wire, a mixed-integer nonlinear programming (MINLP) formulation is used. The binary part of this MINLP model corresponds to the decision variables regarding the connection of a particular monopolar load at node $k$ in the positive or negative pole. The continuous component of the MINLP model has to do with voltage magnitudes, line currents, and power injections, among other variables. The MINLP model that represents the pole-swapping problem is presented below.

### 2.1. Objective Function

The objective function of the optimal pole-swapping problem is the minimization of the total power losses in all distribution lines for the positive, negative, and neutral conductors. Equation (1) defines its formulation.

$$\min p_{\text{loss}} = \sum_{r\in\mathcal{P}} \sum_{j\in\mathcal{N}} V_j^r \left( \sum_{s\in\mathcal{P}} \sum_{k\in\mathcal{N}} G_{jk}{}^{rs} V_k^s \right), \tag{1}$$

where $p_{\text{loss}}$ is the objective function value associated with the total power losses of the grid.

### 2.2. Set of Constraints

The set of constraints associated with the optimal pole-swapping problem contains the power balance in all nodes of the network at each pole and the voltage regulation bounds and conditions of the binary variables, among others. The complete set of constraints is listed in Equations (2) to (16).

$$I_{g,k}^{p} - I_{d,k}^{p} - I_{d,k}^{p-n} = \sum_{r\in\mathcal{P}}\sum_{j\in\mathcal{N}} G_{jk}^{pr} V_k^r, \; \{\forall k \in \mathcal{N}\} \tag{2}$$

$$I_{g,k}^{o} - I_{d,k}^{o} - I_{d,k}^{\text{ground}} = \sum_{r\in\mathcal{P}}\sum_{j\in\mathcal{N}} G_{jk}^{or} V_k^r, \; \{\forall k \in \mathcal{N}\} \tag{3}$$

$$I_{g,k}^{n} - I_{d,k}^{n} + I_{d,k}^{p-n} = \sum_{r\in\mathcal{P}}\sum_{j\in\mathcal{N}} G_{jk}^{nr} V_k^r, \; \{\forall k \in \mathcal{N}\} \tag{4}$$

$$I_{d,k}^{p} = \frac{x_k^p P_{d,k}^p}{V_k^p - V_k^o} + \frac{x_k^n P_{d,k}^n}{V_k^p - V_k^o}, \; \{\forall k \in \mathcal{N}\} \tag{5}$$

$$I_{d,k}^{n} = \frac{x_k^n P_{d,k}^p}{V_k^n - V_k^o} + \frac{x_k^p P_{d,k}^n}{V_k^n - V_k^o}, \; \{\forall k \in \mathcal{N}\} \tag{6}$$

$$I_{d,k}^{o} = \frac{x_k^p P_{d,k}^p + x_k^n P_{d,k}^n}{V_k^o - V_k^p} + \frac{x_k^n P_{d,k}^p + x_k^p P_{d,k}^n}{V_k^o - V_k^n}, \; \{\forall k \in \mathcal{N}\} \tag{7}$$

$$I_{d,k}^{p-n} = \frac{P_{d,k}^{p-n}}{V_k^p - V_k^n}, \; \{\forall k \in \mathcal{N}\} \tag{8}$$

$$I_{g,k}^{p,\min} \le I_{g,k}^{p} \le I_{g,k}^{p,\max}, \; \{\forall k \in \mathcal{N}\} \tag{9}$$

$$I_{g,k}^{o,\min} \le I_{g,k}^{o} \le I_{g,k}^{o,\max}, \; \{\forall k \in \mathcal{N}\} \tag{10}$$

$$I_{g,k}^{n,\min} \le I_{g,k}^{n} \le I_{g,k}^{n,\max}, \; \{\forall k \in \mathcal{N}\} \tag{11}$$

$$V^{p,\min} \le V_k^p \le V^{p,\max}, \; \{\forall k \in \mathcal{N}\} \tag{12}$$

$$V^{n,\min} \le V_k^n \le V^{n,\max}, \; \{\forall k \in \mathcal{N}\} \tag{13}$$

$$\begin{bmatrix} V_j^p \\ V_j^o \\ V_j^n \end{bmatrix} = \begin{bmatrix} 1 \\ 0 \\ -1 \end{bmatrix} V_{\text{nom}}, \; \{j = \text{slack}\} \tag{14}$$

$$x_k^p + x_k^n = 1, \; \{\forall k \in \mathcal{N}\} \tag{15}$$

$$\left\{x_k^p, x_k^n\right\} \in \{0,1\}. \; \{\forall k \in \mathcal{N}\} \tag{16}$$

Note that Equations (2)–(4) correspond to the current injection balance at each node of the network for the positive, negative, and neutral poles. It is important to highlight that these equations are applicable for grids with neutral solidly grounded wire in all nodes of the network or the neutral wire that is only grounded at the substation bus and floating in all remaining nodes. In other operation scenarios, it is necessary to consider the effect of grounding resistance in Equation (3), as presented in [13] for three-phase four-wire distribution networks. Equations (5) to (8) define the current calculation for each pole with its hyperbolic relation between powers and currents. These equations demonstrate the effect of monopolar loads on the total current absorbed from the positive and negative poles. Note that these equations are nonlinear and non-convex, and they require specialized solution methods, which motivates this research to propose a master–slave optimization method based on metaheuristic optimizers and specialized power flow tools for unbalanced bipolar DC networks in order to solve the pole-swapping problem as presented in Section 3. An important fact in Equation (8) is that the effect of bipolar loads is only present in positive and negative poles (see Equations (5) and (6)), since these loads, as expected, are connected between these poles and are not related to the neutral pole.

The set of box-type constraints (9)–(11) present the current limitations of the generation nodes. It is worth mentioning that, for bipolar DC networks, the power generators are connected between the ideal neutral point and each pole, which is similar to the star connection used for generators in three-phase networks. In addition, current injection at the neutral pole for generators is assumed to be equal to zero, which implies that, in constraint (10), $I_{g,k}^{o,\min} = I_{g,k}^{o,\max} = 0$. Box-type constraints (12) and (13) define the voltage regulation limits imposed by regulatory policies to distribution system operators. Note that, in the case of the neutral pole, there is no assigned constraint, since, ideally speaking (in a solidly grounded scenario), all the voltages in this pole must be zero. Equation (14) shows the voltage profiles set in the slack source, with is ideally operated for the positive, neutral, and negative poles. Equation (15) defines that only one binary variable per node is activated in order to determine which load is connected to the positive or negative pole. Note that, if $x_k^p$ is activated, i.e., $x_k^p = 1$, the original load connection is maintained; whereas, if $x_k^n = 1$, the positive and negative monopolar loads are interchanged. Finally, constraint (16) defines the binary nature of the decision variables $x_k^p$ and $x_k^n$.

**Remark 1.** *The solution of the MINLP model (1)–(16) requires efficient methodologies that can deal with the nonlinearities and non-convexities of the solution space given by the hyperbolic relations between voltages and powers in Equations (5)–(9).*

This research presents a master–slave optimization approach based on discrete metaheuristics combined with the bipolar power flow solution approach based on the upper triangular power flow method [9]. The solution methodologies implemented are presented in the next section.

## 3. Solution Methodology

In order to deal with the MINLP formulation given in Equations (1)–(16), the application of a master–slave optimization approach is proposed, which is based on discrete metaheuristic optimizers and a specialized bipolar power flow solver.

### 3.1. Codification

The main advantage of using combinatorial optimization methods to deal with the optimal pole-swapping problem in bipolar DC networks is that with a simple binary codification, it is possible to represent the solution space. This binary codification is presented below.

$$X_i^t = [0,\ ,1,\ 1,\ \cdots 0], \tag{17}$$

where $X_i^t$ corresponds to solution individual $i$ in iteration $t$. Note that the dimension of the solution space for this problem is $2^{n-1}$ [14], with $n$ being the total number of nodes of the bipolar DC network. It is important to highlight that a value of 0 in Equation (17) means that $x_k^p = 1$ and $x_k^n = 0$, and a value of 1 means that $x_k^p = 0$ and $x_k^n = 1$.

### 3.2. Slave Stage: Power Flow Solution Approach

The heart of any master–slave optimization method corresponds to the slave stage, as it typically aims to define the technical feasibility of each solution vector $x_i^t$ provided by the master optimization methodology. This study adopts a recent power flow formulation derived specifically for bipolar DC networks with a radial structure. This is a derivative free power flow formulation based on the upper triangular matrix that relates the nodal injected currents with the branch currents [9].

The triangular-based power flow formula is presented in Equation (18). This power flow formula is derived by applying the graph theory for radial distribution networks presented by [15].

$$V_d^{pon,m+1} = \mathbf{A}_{ds} V_s^{pon} - \mathbf{R}_{dd}^{pon} I_d^{pon,m}. \tag{18}$$

where $V_d^{pon,m+1}$ is the vector that contains all the demand voltages at iteration $m+1$ for the positive, neutral, and negative poles, respectively, which is a nonlinear function of the demanded currents currents $I_d^{pon,m}$. In addition, $V_s^{pon}$ represents the voltage outputs in the substation (see Equation (14)). Note that $\mathbf{A}_{ds}$ and $\mathbf{R}_{dd,pon}$ are matrices that depend on the grid topology under analysis. Note that the demanded currents $I_d^{pon,m}$ remain in the form of a hyperbolic relation between voltages and powers, and they also depend on the binary variables $x_k^p$ and $x_k^n$, i.e., they are a function of the decision vector $X_i^t$. Note that $I_{d,k}^{pon,m}$ for each node $k$ can be defined as presented in Equation (19).

$$I_{dk}^{pon,m} = \mathbf{H}\text{diag}^{-1}\left(\Delta v_{dk}^{pon,m}\right)\mathbf{X}_k P_{dk}^{pon}, \tag{19}$$

where

$$I_{d,k}^{pon,m} = \begin{bmatrix} i_{d,k}^p \\ i_{d,k}^o \\ i_{d,k}^n \end{bmatrix}, \mathbf{H} = \begin{bmatrix} 1 & 1 & 0 \\ -1 & 0 & -1 \\ 0 & -1 & 1 \end{bmatrix}, P_{dk}^{pon} = \begin{bmatrix} p_{d,k}^p \\ p_{d,k}^{p-n} \\ p_{d,k}^n \end{bmatrix}.$$

where $v_{d,k}^{po} = v_{d,k}^p - v_{d,k}^o$, $v_{d,k}^{pn} = v_{d,k}^p - v_{d,k}^n$, and $v_{d,k}^{no} = v_{d,k}^n - v_{d,k}^n$ are grouped into a vector as $\Delta v_{d,k}^{pon} = [v_{d,k}^{po}, v_{d,k}^{pn}, v_{d,k}^{no}]^\top$. It is worth mentioning that $\mathbf{X}_k$ represents the monopolar load connections at node $k$, i.e., it is the variable that decodes the solution value for each node contained in $X_i^t$. The decodification for each node $k$ is presented below:

$$X_{i,k}^t = 0 \rightarrow \begin{bmatrix} x_k^p \\ x_k^n \end{bmatrix} = \begin{bmatrix} 1 \\ 0 \end{bmatrix} \rightarrow \mathbf{X}_k = \begin{bmatrix} 1 & 0 & 0 \\ 0 & 1 & 0 \\ 0 & 0 & 1 \end{bmatrix}, \tag{20}$$

$$X_{i,k}^t = 1 \rightarrow \begin{bmatrix} x_k^p \\ x_k^n \end{bmatrix} = \begin{bmatrix} 0 \\ 1 \end{bmatrix} \rightarrow \mathbf{X}_k = \begin{bmatrix} 0 & 0 & 1 \\ 0 & 1 & 0 \\ 1 & 0 & 0 \end{bmatrix}. \tag{21}$$

**Remark 2.** *The mathematical structure of the decodification variable $X_k$ shows that the bipolar DC constant power terminals remain unaltered by the pole-swapping solution since these are connected between the positive and negative poles and are not related to the neutral wire.*

To determine when the power flow solution Formula (18) has converged to the power flow solution, the maximum difference between two consecutive iterations is determined, i.e., $\max\left\{||V_d^{pon,m+1}| - |V_d^{pon,m}||\right\} \leq \zeta$, with zeta being the maximum convergence error, which is typically chosen as $1 \times 10^{-10}$ [9].

Once the power flow problem is solved for each solution vector $X_i^t$, the total grid power losses for this configuration can be obtained, which are calculated as defined in Equation (22).

$$p_{\text{loss}} = J_l^{pon,\top} \mathbf{R}_{ll}^{pon} J_l^{pon}, \tag{22}$$

where $J_l^{pon,\top}$ represents the vector with all the currents through the lines, and $\mathbf{R}_{ll}^{pon}$ is the primitive resistance matrix associated with all the branches.

**Remark 3.** *For additional information regarding the triangular-based power flow formulation for bipolar DC networks with strictly radial configurations, see [9,15].*

### 3.3. Master Stage: Metaheuristic Optimizers

The master stage corresponds to the brain of the optimization methodology since it is entrusted with guiding the exploration and exploitation of the solution space by means of specialized evolution rules. In this research, three combinatorial optimization methods are studied in order to solve the optimal pole-swapping problem in bipolar DC networks. As previously discussed, these are the Chu and Beasley genetic algorithm (CBGA), the sine-cosine algorithm (SCA), and the black-hole optimizer (BHO).

**Remark 4.** *The selection of the CGBA, the SCA, and the BHO considered that each one of them comes from a different optimization family, with the AGCB being inspired by nature [16], the SCA by mathematics [17], and the BHO by physics [18].*

The main characteristic of these algorithms is that they work with an initial population, i.e., a set of candidate solutions conformed by a matrix with rows of the same form as the codification vector in Equation (17). A brief explanation of these algorithms is presented below.

#### 3.3.1. Chu Beasley Genetic Algorithm

Genetic algorithms are probably the most popular optimization algorithms to deal with multiple combinatorial optimization problems. They were initially developed during the 1970s by Holland [19], with the objective of solving complex optimization problems, inspired by the theory of natural selection proposed by Charles Darwin. The CGBA is a population-based optimizer that works with an initial population that evolves using three simple rules: (i) selection, (ii) recombination, and (iii) mutation.

- ✓ **Selection:** in this stage, two arbitrary solution individuals are chosen from the population, i.e., $X_i^t$ and $X_j^t$, where the only constraint is that $i$ and $j$ must be different. These individuals are known as the *parents*.
- ✓ **Recombination:** in this stage, the genetic information of both individuals is mixed using a recombination point in order to obtain two new individuals, which are called offspring.
- ✓ **Mutation:** in this stage, each offspring is randomly mutated by changing its genetic information in a particular position using probabilities, which emulates the differences between sons from the same family, even if both come from the same parents.

Once the offspring population is generated, both are evaluated using the slave stage, and only one of them has the right to be part of the population, i.e., if it is better than the worst individual in the population and it meets the diversity criteria.

#### 3.3.2. Sine-Cosine Algorithm

The sine-cosine optimization algorithm corresponds to a mathematically inspired optimizer that uses two evolution rules based on the trigonometric functions of sine and cosine in order to explore and exploit the solution space. This algorithm was initially developed by the authors of [20] to solve the optimal power flow problem in power systems with multiple thermal generation plants. The evolution rule applied for an individual $X_i^t$ contained in the population is presented in Equation (23).

$$Y_i^{t+1} = \begin{cases} \text{round}\left(X_i^t + r_1 \sin(r_2)\left|r_3 X_i^t - X^{t,\text{best}}\right|\right) & r_4 \geq \frac{1}{2} \\ \text{round}\left(X_i^t + r_1 \cos(r_2)\left|r_3 X_i^t - X^{t,\text{best}}\right|\right) & r_4 < \frac{1}{2} \end{cases} \tag{23}$$

where $r_1$ is a parameter that represents the importance of evolution of the sine and cosine, which is defined as a function of the number of iterations, i.e., $r_1 = 1 - \frac{t}{t_{\max}}$, with $t_{\max}$ being the maximum number of iterations. $r_2$ is a random number with uniform distribution contained in the interval between $[0, 2pi]$. $r_3$ and $r_4$ are random numbers with uniform distribution contained in the interval between $[0, 1]$, and $X^{t,\text{best}}$ represents the best current solution contained in the current population.

Note that once the evolution rule is applied for each individual $X_i^t$ in order to generate the next solution individual $X_i^{t+1}$, it is mandatory to check if all the components of this vector are binary. Otherwise, these are corrected by generating a random binary number to replace the incorrect value. Note that this revision stage is fundamental for maintaining a feasible solution space for the pole-swapping problem.

**Remark 5.** *The inclusion of the new potential solution $Y_i^{t+1}$ in the current population is performed only if it is better than the current solution, i.e.,:*

- $X^{t+1} = Y_i^{t+1}$ *if and only if* $p_{loss}\left(Y_i^{t+1}\right) < p_{loss}\left(X_i^t\right)$.
- *Otherwise,* $X^{t+1} = X_i^t$.

3.3.3. Black Hole Optimizer

The BHO is a physically inspired optimization algorithm based on the physical interaction between black holes and stars at the center of galaxies [21]. The BHO has three important characteristics regarding its exploration and exploitation of the solution space [22].

i. The location of the black hole corresponds to the best current solution in the population, i.e., $X^{t,\text{best}}$;
ii. the movements of the stars (remaining solution individuals in the population) are influenced by their current positions and the gravitational force exerted by the black hole;
iii. the stars that surpass the event horizon are absorbed by the black hole (destroyed), and, with stellar gas around the black hole, a new star is created.

The evolution rule in the BHO takes the form presented in Equation (24).

$$Y_i^{t+1} = \text{round}\left(X_i^t + r_i\left(X^{\text{best}-X_i^t}\right)\right), \tag{24}$$

where $r_i$ is a vector with the same dimensions of the individual $X_i^t$ filled by values between 0 and 1 with a uniform distribution that includes pondering the effect of the black hole on the next solution. Like the SCA algorithm, the feasibility of each component in the potential solution $Y_i^{t+1}$ is verified and corrected when necessary in order to keep the solution space feasible. In addition, the same replacement criterion is applied.

In case the new individual $Y_i^{t+1}$ surpasses the event horizon, a new star is randomly generated with the same structure, as defined in Equation (17). For additional details regarding the implementation of the BHO, see [22,23].

### *3.4. Summary of the Metaheuristic Optimization Methodologies*

The application of the CBGA, the SCA, or the BHO to solve the optimal pole-swapping problem in bipolar DC networks with multiple constant power terminals is summarized in Algorithm 1.

**Algorithm 1:** Proposed master–slave optimization approach to solve the optimal pole-swapping problem in bipolar DC networks.

**Data:** Select the bipolar DC network under analysis
Find the per-unit equivalent representation of the network;
Define the number of iterations $t_{\max}$ for the metaheuristic algorithms;
Make $t = 0$;
Select the size of the initial population, i.e., $X^0$;
Define the number of iterations $m_{\max}$ for the power flow problem;
Define the tolerance of the power flow problem, i.e., $\zeta = 1 \times 10^{-10}$;
Evaluate each individual $X_i^t$ in the power flow formulas of Equations (18) and (19);
**for** $t = 1 : t_{\max}$ **do**
  **if** *Selected method* $=$ *CBGA* **then**
    Select two arbitrary parents $X_i^t$ and $X_j^t$;
    Recombine both parents to obtain two offspring individuals;
    Apply the mutation operator to each offspring;
    Evaluate each offspring in the power flow formulas of Equations (18) and (19); Select the winning individual;
    **if** *Is the winner better than the worst individual in the population?* **then**
      **if** *Is the winner different from all the individuals in the population?* **then**
        Replace the worst individual with the winner;
      **end**
    **end**
  **end**
  **if** *Selected method* $=$ *SCA* **then**
    Generate random values for $r_2$, $r_3$, and $r_4$, and calculate $r_1 = 1 - \frac{t}{t_{max}}$;
    Apply evolution rule in Formula (23) to obtain $Y_i^{t+1}$;
    Revise/correct the feasibility of the potential solution $Y_i^{t+1}$;
    Evaluate $Y_i^{t+1}$ in the power flow formulas of Equations (18) and (19);
    **if** $p_{loss}\left(Y_i^{t+1}\right) < p_{loss}\left(X_i^t\right)$ **then**
      Replace $X_i^{t+1}$ with $Y_i^{t+1}$;
    **else**
      Make $X_i^{t+1} = Y_i^t$;
    **end**
  **end**
  **if** *Selected method* $=$ *BHO* **then**
    Generate random values for $r_1$;
    Apply evolution rule in Formula (24) to obtain $Y_i^{t+1}$;
    Revise/correct the feasibility of the potential solution $Y_i^{t+1}$;
    Evaluate $Y_i^{t+1}$ in the power flow formulas of Equations (18) and (19);
    **if** $p_{loss}\left(Y_i^{t+1}\right) < p_{loss}\left(X_i^t\right)$ **then**
      Replace $X_i^{t+1}$ with $Y_i^{t+1}$;
    **end**
    Make $X_i^{t+1} = Y_i^t$;
  **end**
**end**
Order all solutions in ascending form with the values of the objective function;
**Result:** Report the optimal solution

Note that, in order to compare all of the metaheuristic optimizers, the same number of individuals in the population is evaluated, as well as in the same number of iterations. In addition, each method is evaluated 100 times to obtain its statistical behavior.

## 4. Test Feeder Characteristics

To validate the proposed optimization methodology, two test feeders composed of 21 and 85 buses were used. The electrical information for both test feeders is presented below.

### *4.1. The 21-Bus System*

This test feeder corresponds to an adaptation of the original monopolar DC distribution grid proposed in [24] to evaluate the convergence of the Newton–Raphson method in power flow studies involving DC networks. The grid topology of this test feeder is depicted in Figure 1.

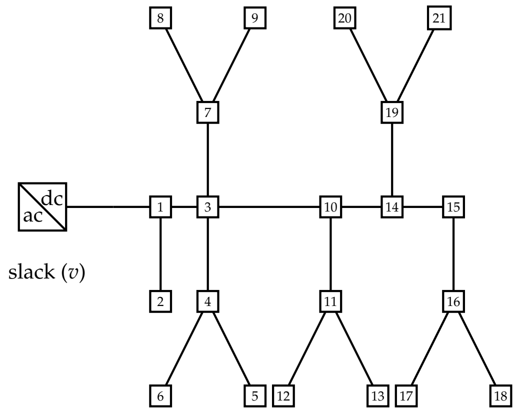


**Figure 1.** Grid configuration of the 21-bus system.

The main characteristics of this test feeder are as follows: (i) it has a radial configuration; (ii) the substation is located at node 1, which is operated with $\pm 1$ kV for the positive and negative poles while the neutral pole is assigned 0 V; (iii) the total monopolar loads amount to 554 kW in the positive pole and 445 kW in the negative pole. The complete parametric information for this test feeder is listed in Table 1.

**Table 1.** Data for the 21-bus system (all powers in kW).

| Node $j$ | Node $k$ | $R_{jk}$ ($\Omega$) | $P_{d,k}^{p}$ | $P_{d,k}^{n}$ | $P_{d,k}^{p-n}$ |
|---|---|---|---|---|---|
| 1 | 2 | 0.053 | 70 | 100 | 0 |
| 1 | 3 | 0.054 | 0 | 0 | 0 |
| 3 | 4 | 0.054 | 36 | 40 | 120 |
| 4 | 5 | 0.063 | 4 | 0 | 0 |
| 4 | 6 | 0.051 | 36 | 0 | 0 |
| 3 | 7 | 0.037 | 0 | 0 | 0 |
| 7 | 8 | 0.079 | 32 | 50 | 0 |
| 7 | 9 | 0.072 | 80 | 0 | 100 |
| 3 | 10 | 0.053 | 0 | 10 | 0 |
| 10 | 11 | 0.038 | 45 | 30 | 0 |
| 11 | 12 | 0.079 | 68 | 70 | 0 |
| 11 | 13 | 0.078 | 10 | 0 | 75 |
| 10 | 14 | 0.083 | 0 | 0 | 0 |
| 14 | 15 | 0.065 | 22 | 30 | 0 |

**Table 1.** *Cont.*

| Node $j$ | Node $k$ | $R_{jk}$ ($\Omega$) | $P_{d,k}^{p}$ | $P_{d,k}^{n}$ | $P_{d,k}^{p-n}$ |
|---|---|---|---|---|---|
| 15 | 16 | 0.064 | 23 | 10 | 0 |
| 16 | 17 | 0.074 | 43 | 0 | 60 |
| 16 | 18 | 0.081 | 34 | 60 | 0 |
| 14 | 19 | 0.078 | 9 | 15 | 0 |
| 19 | 20 | 0.084 | 21 | 10 | 50 |
| 19 | 21 | 0.082 | 21 | 20 | 0 |

*4.2. The 85-Bus System*

The 85-bus grid corresponds to an equivalent of the classical IEEE 85-bus grid presented in [25] for the optimal placement of capacitor banks. This adaptation was proposed by the authors of [9] for the application of the triangular-based power flow formulation in imbalanced bipolar DC networks. The electrical topology for the 85-bus grid is depicted in Figure 2.

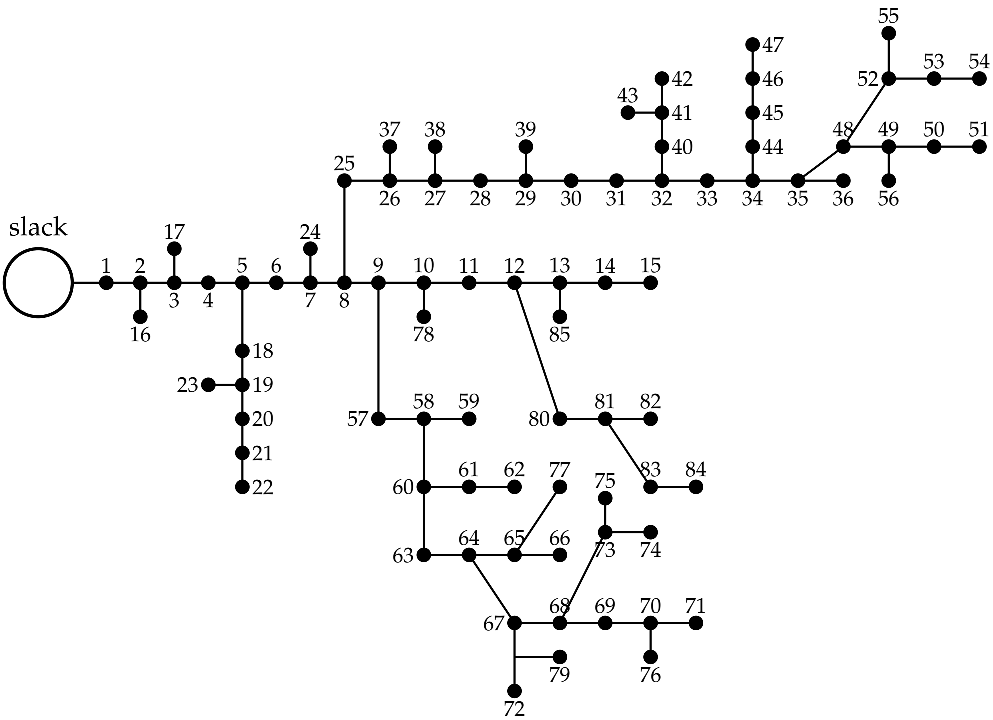


**Figure 2.** Electrical configuration of the 85-bus system for bipolar DC network analysis.

The information regarding the branch and load parameters for this test feeder is reported in Table 2. Note that this system is operated with ±11 kV in the positive and negative poles, while the neutral wire at the substation is set to 0 V.

**Table 2.** Data for the 85-bus system (all powers in kW).

| Node $j$ | Node $k$ | $R_{jk}$ (Ω) | $P^{p}_{d,k}$ | $P^{n}_{d,k}$ | $P^{p-n}_{d,k}$ | Node $j$ | Node $k$ | $R_{jk}$ (Ω) | $P^{p}_{d,k}$ | $P^{n}_{d,k}$ | $P^{p-n}_{d,k}$ |
|---|---|---|---|---|---|---|---|---|---|---|---|
| 1 | 2 | 0.108 | 0 | 0 | 10.075 | 34 | 44 | 1.002 | 17.64 | 17.995 | 0 |
| 2 | 3 | 0.163 | 50 | 0 | 40.35 | 44 | 45 | 0.911 | 50 | 17.64 | 17.995 |
| 3 | 4 | 0.217 | 28 | 28.565 | 0 | 45 | 46 | 0.911 | 25 | 17.64 | 17.995 |
| 4 | 5 | 0.108 | 100 | 50 | 0 | 46 | 47 | 0.546 | 7 | 7.14 | 10 |
| 5 | 6 | 0.435 | 17.64 | 17.995 | 25.18 | 35 | 48 | 0.637 | 0 | 10 | 0 |
| 6 | 7 | 0.272 | 0 | 8.625 | 0 | 48 | 49 | 0.182 | 0 | 0 | 25 |
| 7 | 8 | 1.197 | 17.64 | 17.995 | 30.29 | 49 | 50 | 0.364 | 18.14 | 0 | 18.505 |
| 8 | 9 | 0.108 | 17.8 | 350 | 40.46 | 50 | 51 | 0.455 | 28 | 28.565 | 0 |
| 9 | 10 | 0.598 | 0 | 100 | 0 | 48 | 52 | 1.366 | 30 | 0 | 15 |
| 10 | 11 | 0.544 | 28 | 28.565 | 0 | 52 | 53 | 0.455 | 17.64 | 35 | 17.995 |
| 11 | 12 | 0.544 | 0 | 40 | 45 | 53 | 54 | 0.546 | 28 | 30 | 28.565 |
| 12 | 13 | 0.598 | 45 | 40 | 22.5 | 52 | 55 | 0.546 | 38 | 0 | 48.565 |
| 13 | 14 | 0.272 | 17.64 | 17.995 | 35.13 | 49 | 56 | 0.546 | 7 | 40 | 32.14 |
| 14 | 15 | 0.326 | 17.64 | 17.995 | 20.175 | 9 | 57 | 0.273 | 48 | 35.065 | 10 |
| 2 | 16 | 0.728 | 17.64 | 67.5 | 33.49 | 57 | 58 | 0.819 | 0 | 50 | 0 |
| 3 | 17 | 0.455 | 56.1 | 57.15 | 50.25 | 58 | 59 | 0.182 | 18 | 28.565 | 25 |
| 5 | 18 | 0.820 | 28 | 28.565 | 200 | 58 | 60 | 0.546 | 28 | 43.565 | 0 |
| 18 | 19 | 0.637 | 28 | 28.565 | 10 | 60 | 61 | 0.728 | 18 | 28.565 | 30 |
| 19 | 20 | 0.455 | 17.64 | 17.995 | 150 | 61 | 62 | 1.002 | 12.5 | 29.065 | 0 |
| 20 | 21 | 0.819 | 17.64 | 70 | 152.5 | 60 | 63 | 0.182 | 7 | 7.14 | 5 |
| 21 | 22 | 1.548 | 17.64 | 17.995 | 30 | 63 | 64 | 0.728 | 0 | 0 | 50 |
| 19 | 23 | 0.182 | 28 | 75 | 28.565 | 64 | 65 | 0.182 | 12.5 | 25 | 37.5 |
| 7 | 24 | 0.910 | 0 | 17.64 | 17.995 | 65 | 66 | 0.182 | 40 | 48.565 | 33 |
| 8 | 25 | 0.455 | 17.64 | 17.995 | 50 | 64 | 67 | 0.455 | 0 | 0 | 0 |
| 25 | 26 | 0.364 | 0 | 28 | 28.565 | 67 | 68 | 0.910 | 0 | 0 | 0 |
| 26 | 27 | 0.546 | 110 | 75 | 175 | 68 | 69 | 1.092 | 13 | 18.565 | 25 |
| 27 | 28 | 0.273 | 28 | 125 | 28.565 | 69 | 70 | 0.455 | 0 | 20 | 0 |
| 28 | 29 | 0.546 | 0 | 50 | 75 | 70 | 71 | 0.546 | 17.64 | 38.275 | 17.995 |
| 29 | 30 | 0.546 | 17.64 | 0 | 17.995 | 67 | 72 | 0.182 | 28 | 13.565 | 0 |
| 30 | 31 | 0.273 | 17.64 | 17.995 | 0 | 68 | 73 | 1.184 | 30 | 0 | 0 |
| 31 | 32 | 0.182 | 0 | 175 | 0 | 73 | 74 | 0.273 | 28 | 50 | 28.565 |
| 32 | 33 | 0.182 | 7 | 7.14 | 12.5 | 73 | 75 | 1.002 | 17.64 | 6.23 | 17.995 |
| 33 | 34 | 0.819 | 0 | 0 | 0 | 70 | 76 | 0.546 | 38 | 48.565 | 0 |
| 34 | 35 | 0.637 | 0 | 0 | 50 | 65 | 77 | 0.091 | 7 | 17.14 | 25 |
| 35 | 36 | 0.182 | 17.64 | 0 | 17.995 | 10 | 78 | 0.637 | 28 | 6 | 28.565 |
| 26 | 37 | 0.364 | 28 | 30 | 28.565 | 67 | 79 | 0.546 | 17.64 | 42.995 | 0 |
| 27 | 38 | 1.002 | 28 | 28.565 | 25 | 12 | 80 | 0.728 | 28 | 28.565 | 30 |
| 29 | 39 | 0.546 | 0 | 28 | 28.565 | 80 | 81 | 0.364 | 45 | 0 | 75 |
| 32 | 40 | 0.455 | 17.64 | 0 | 17.995 | 81 | 82 | 0.091 | 28 | 53.75 | 0 |
| 40 | 41 | 1.002 | 10 | 0 | 0 | 81 | 83 | 1.092 | 12.64 | 32.995 | 62.5 |
| 41 | 42 | 0.273 | 17.64 | 25 | 17.995 | 83 | 84 | 1.002 | 62 | 72.2 | 0 |
| 41 | 43 | 0.455 | 17.64 | 17.995 | 0 | 13 | 85 | 0.819 | 10 | 10 | 10 |

## 5. Numerical Validations

The computational implementation of the metaheuristic methodologies for solving the optimal pole-swapping problem in bipolar DC networks with multiple constant monopolar and bipolar loads was executed in the MATLAB programming environment using the researchers' own scripts. For this implementation, version 2021*b* was used on a PC with an AMD Ryzen 7 3700 2.3 GHz processor and 16.0 GB RAM, running on a 64-bit version of Microsoft Windows 10 Single Language.

In the numerical simulations, it was considered that the neutral wire was only grounded at the substation bus, since, as demonstrated by [9], this is the worst scenario regarding power losses when compared to the solidly grounded case for all the nodes of the network.

## 6. Results in the 21-Bus System

The solution to the pole-swapping problem for the 21-bus grid with the CBGA, the SCA, and the BHO is presented in Table 3.

**Table 3.** Results of the 21-bus system for the proposed metaheuristic optimizers.

| Method | Nodes with Modification | $p_{\text{loss}}$ (kW) | Reduction (%) | Time (s) |
|---|---|---|---|---|
| Benchmark case | — | 95.4237 | — | — |
| SCA | $[4, 6, 11, 16, 21]$ | 91.6630 | 3.9413 | 8.8340 |
| BHO | $[3, 5, 7, 8, 9, 10, 12, 13, 16, 21]$ | 91.6628 | 3.9411 | 16.2323 |
| CBGA | $[5, 7, 8, 9, 10, 12, 13, 14, 16, 21]$ | 91.6628 | 3.9411 | 2.2620 |

The numerical results in Table 3 show that:

i. The expected power losses reduction after applying each one of the metaheuristic optimizers is about 3.9411% with respect to the benchmark case, i.e., there is a net reduction of 3.7609 kW.
ii. The total processing times were considerably lower in the case of the CBGA since it only took about 202,620 s to solve the pole-swapping problem, whereas the SCA took about 8.8340 s in the second position. This makes the BHO the worst algorithm regarding processing times, with a mean duration of 16.2323 s.
iii. The solution provided by the SCA shows that the solution only requires changes in five nodes, with an objective function value of 91.6630 kW, while the BHO and the CBGA make changes in ten nodes. Note that, for all three optimization methods, nodes 16 and 21 were identified in the final solution. In addition, the solutions provided by the BHO and the CBGA have nodes 5, 7, 8, 9, 10, 12, 13, 16, and 21 in both solutions, and they only interchange nodes 3 and 14. However, the latter do not have loads, which confirms that the solutions provided by the BHO and the CBGA are identical.

On the other hand, Figure 3 presents the behavior of the voltage profiles in all the nodes of the 21-bus system for each pole, considering the benchmark case as well as the solution reached with each one of the metaheuristic optimizers.

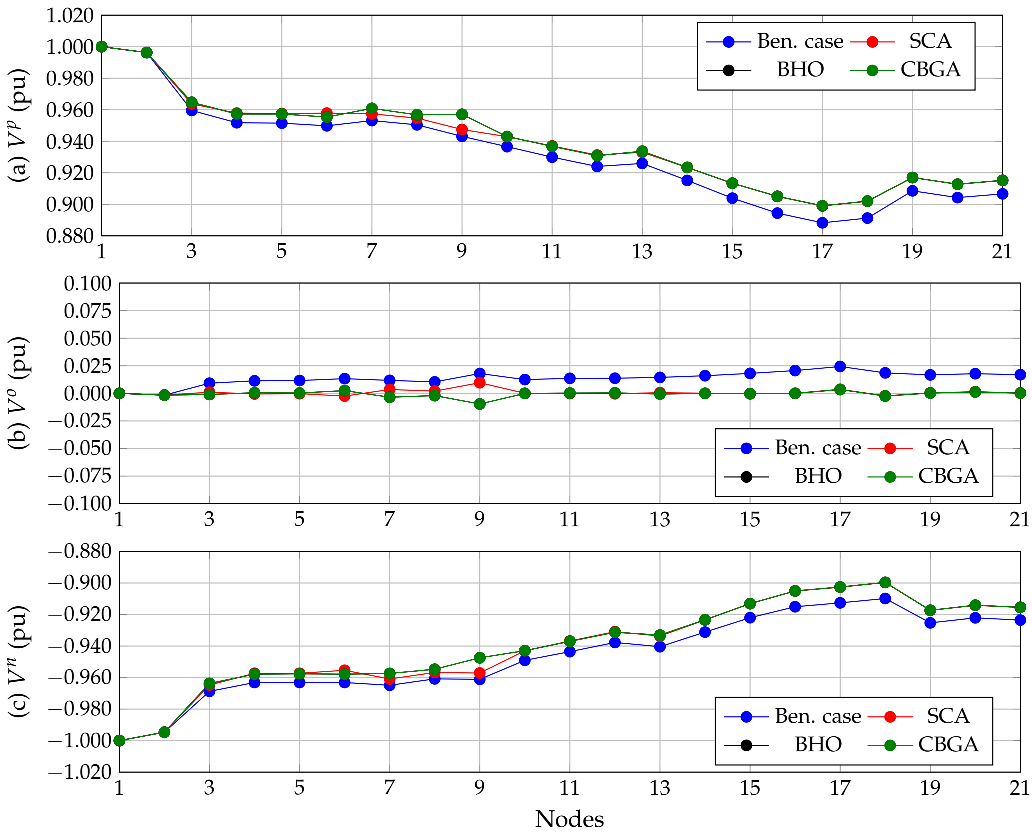


**Figure 3.** Behavior of the voltages for all poles in the 21-bus systems with each one of the metaheuristic optimizers: (**a**) voltage value at the positive pole, (**b**) voltage value at the neutral pole, and (**c**) voltage value at the negative pole.

The main result in Figure 3 is the positive effect of pole-swapping on the voltage behavior of all nodes in the network for each pole. When the voltage profiles in the positive poles are compared to those in the negative pole, it is observed that the system was balanced, which implies that the pole with the highest loadability will increase due to the load reduction on it (see Figure 3a), at the same time that, in the pole with less it will decrease as a function of its load increment. Note that the most positive effect on the optimal pole swapping is in the neutral wire since the deviation with respect to the ideal voltage is reduced when compared with the benchmark case, as can be seen in Figure 3c.

## 7. Results in the 85-Bus System

The solution to the pole-swapping problem for the 85-bus grid with the CBGA, the SCA, and the BHO is presented in Table 4. Note that the benchmark case for this test feeder, as reported in [9], has an initial power loss value of 489.5759 kW.

**Table 4.** Results in the 85-bus system for the proposed metaheuristic optimizers.

| Method | Nodes with Modification | $p_{loss}$ (kW) | Reduction (%) | Time (s) |
|---|---|---|---|---|
| Ben. case | — | 489.5759 | — | — |
| SCA | $\begin{bmatrix} 6,8,9,12,13,14,15,17,19,22,23,30, \\ 32,33,34,35,36,37,40,41,44,45,53, \\ 55,57,59,61,63,65,68,71,81,83 \end{bmatrix}$ | 440.0133 | 10.1236 | 68.4910 |
| BHO | $\begin{bmatrix} 3,6,7,9,11,14,16,17,19,22,23,24,29,31,34, \\ 37,39,43,44,49,55,56,57,61,62,64,65,66,68, \\ 69,71,72,73,74,75,76,78,79,80,81,82,84 \end{bmatrix}$ | 440.1445 | 10.0968 | 133.2345 |
| CBGA | $\begin{bmatrix} 2,4,5,9,12,13,18,19,20,22,23,29,31,33,34, \\ 35,38,39,42,43,44,46,47,48,51,53,54,55,57, \\ 62,70,72,73,74,76,77,78,79,80,81,82,84,85 \end{bmatrix}$ | 439.8161 | 10.1639 | 15.5741 |

The numerical results in Table 4 allow one to observe that:

i. The expected reductions in the power losses for the 85-bus grid are between 10.1639 and 10.0968%, i.e., a final power loss value of 439.8161 kW was obtained for the CBGA and 440.1445 kW for the BHO.
ii. In numerical terms, all the three explored metaheuristic optimizers find adequate values for the objective function, with a difference of 0.3284 kW between them, which implies that the SCA and the BHO methods reach near-optimal solutions with respect to the solution found with the CBGA.
iii. The solution found with the SCA proposes the movement of loads in 33 nodes, the BHO moves loads in 43 nodes, and the CBGA also changes connections in 43 nodes. Comparisons between the SCA and the other optimizers show that near-optimal solution values can correspond to very different locations in the solution spaces since the number of interventions in the nodes of the network is 11.76%, which is lower in comparison with the BHO and the CBGA.

*Statistical Evaluation*

To show the effectiveness and robustness of the proposed metaheuristic optimizers when dealing with the problem regarding the optimal pole-swapping problem in bipolar DC networks, 100 consecutive implementations of each optimization algorithm were executed to obtain their maximum, mean, and minimum values, as well as the standard deviations for each test feeder and each metaheuristic optimizer. Table 5 presents the statistical behavior of the CBGA, the BHO, and the SCA for each test feeder.

The results in Table 5 allow us to observe that: (i) for both test feeders, the SCA is the optimization method with the highest variations with respect to the mean value, since the standard deviation is 0.2256 kW for the 21-bus grid and 0.3323 kW for the 85-bus grid, while the best optimization method regarding stability after each execution is the BHO, with standard deviations of 0.0122 and 0.1143 kW for the 21- and 85-bus grids, respectively; (ii) with respect to the maximum value, it is observed that, in both cases the SCA finds the worst solution among the three optimization methods, in comparison with values of 92.7745 and 441.8369 kW; (iii) with respect to the minimum value, it is possible to note that the solution in the 21-bus grids is the same for the BHO and the CBGA, with a minimum objective function of 91.6628 kW, whereas, for the 85-bus grid, only the CBGA obtains a solution of less than 440 kW, followed by the SCA with a value of 440.0133 kW.

**Table 5.** Statistical behavior of the three metaheuristic optimizers in both test feeders after 100 consecutive evaluations.

| Method | Maximum (kW) | Minimum (kW) | Mean (kW) | Stand. Deviation (kW) |
|---|---|---|---|---|
| | | 21-bus grid | | |
| SCA | 92.7745 | 91.6630 | 91.8161 | 0.2256 |
| BHO | 91.7084 | 91.6628 | 91.6784 | 0.0122 |
| CBGA | 91.7461 | 91.6628 | 91.6824 | 0.0190 |
| | | 85-bus grid | | |
| SCA | 441.8369 | 440.0133 | 440.5837 | 0.3323 |
| BHO | 440.6536 | 440.1445 | 440.3452 | 0.1143 |
| CBGA | 440.7200 | 439.8161 | 440.0459 | 0.1542 |

Note that the results in Table 5 confirm that, with respect to the minimum objective function value, the best optimization method is the CBGA. Moreover, regarding the stability of the solution (i.e., the minimum standard deviation) the best method is the BHO.

## 8. Conclusions and Future Works

The problem regarding the optimal pole-swapping problem in bipolar DC networks with multiple monopolar and bipolar constant power terminals was addressed in this research through the application of three solution methodologies with a master–slave structure. In the master stage, a metaheuristic optimizer (CBGA, BHO, or SCA) was employed to define the load connection at each node, while the slave stage was entrusted with evaluating the total grid power losses by using a triangular-based power flow formulation specialized for radial bipolar DC networks.

Numerical results in the 21-bus grid showed that the three optimization methods allow reductions of about 3.94% with respect to the benchmark case, whereas, for the 85-bus grid, these reductions are between 10.10 and 10.16%. In both test feeders, the CBGA finds the best objective function value (minimum value): 91.6628 and 439.8161 kW, respectively.

With respect to the voltage profile performance, as expected, the optimal load redistribution in the positive and negative poles with respect to the benchmark case allows noting that the neutral voltage drop was minimized in the 21-bus system, which made the voltage magnitudes of the positive and negative poles similar in comparison with the benchmark case. The initial differences between total monopolar consumptions in the 21- and 85-bus grids were 109 and 1873.42 kW, respectively, whereas, when the optimal solution found with the CBGA was implemented in both test feeders, these imbalances were reduced to 47 and 52.58 kW, respectively.

The statistical analysis of the three metaheuristic optimizers revealed that: (i) the most stable algorithm after 100 consecutive evaluations was the BHO since it showed a lower standard deviation in both test feeders; (ii) with respect to the final objective function value, the most efficient algorithm was the CBGA since it found the minimum value of the power losses in both test feeders.

As future work, the following studies can be conducted: (i) proposing new metaheuristic optimizers to deal with the optimal pole-swapping problem (i.e., the vortex search algorithm, the generalized normal distribution algorithm, and the gradient-based metaheuristic optimizer, among others); (ii) developing a mixed-integer convex optimization model to reformulate the exact MINLP model given in Equations (1) to (16) in order to ensure that the global optimum is reached via the convex optimization theory.

**Author Contributions:** Conceptualization, methodology, software, and writing (review and editing): O.D.M., Á.M.-Q. and J.C.H. All authors have read and agreed to the published version of the manuscript.

**Funding:** This work was partially supported by the Proyecto Curricular de Ingeniería Eléctrica (Curricular Electrical Engineering Project) attached to the Department of Engineering of Universidad Distrital Franscisco José de Caldas in Bogotá, Colombia.

**Institutional Review Board Statement:** Not applicable.

**Informed Consent Statement:** Not applicable.

**Data Availability Statement:** No new data were created or analyzed in this study. Data sharing is not applicable to this article.

**Conflicts of Interest:** The authors declare no conflict of interest.

## References

1. Garcés, A.; Montoya, O.D. A Potential Function for the Power Flow in DC Microgrids: An Analysis of the Uniqueness and Existence of the Solution and Convergence of the Algorithms. *J. Control. Autom. Electr. Syst.* **2019**, *30*, 794–801. [CrossRef]
2. Mackay, L.; Guarnotta, R.; Dimou, A.; Morales-Espana, G.; Ramirez-Elizondo, L.; Bauer, P. Optimal Power Flow for Unbalanced Bipolar DC Distribution Grids. *IEEE Access* **2018**, *6*, 5199–5207. [CrossRef]
3. Guo, C.; Wang, Y.; Liao, J. Coordinated Control of Voltage Balancers for the Regulation of Unbalanced Voltage in a Multi-Node Bipolar DC Distribution Network. *Electronics* **2022**, *11*, 166. [CrossRef]
4. Garces, A.; Montoya, O.D.; Gil-Gonzalez, W. Power Flow in Bipolar DC Distribution Networks Considering Current Limits. *IEEE Trans. Power Syst.* **2022**, 1–4. [CrossRef]
5. Lee, J.O.; Kim, Y.S.; Jeon, J.H. Generic power flow algorithm for bipolar DC microgrids based on Newton–Raphson method. *Int. J. Electr. Power Energy Syst.* **2022**, *142*, 108357. [CrossRef]
6. Li, B.; Wang, W.; Liu, Y.; Li, B.; Wen, W. Research on power flow calculation method of true bipolar VSC-HVDC grids with different operation modes and control strategies. *Int. J. Electr. Power Energy Syst.* **2021**, *126*, 106558. [CrossRef]
7. Tavakoli, S.D.; Khajesalehi, J.; Hamzeh, M.; Sheshyekani, K. Decentralised voltage balancing in bipolar dc microgrids equipped with trans-z-source interlinking converter. *IET Renew. Power Gener.* **2016**, *10*, 703–712. [CrossRef]
8. Liao, J.; You, X.; Liu, H.; Huang, Y. Voltage stability improvement of a bipolar DC system connected with constant power loads. *Electr. Power Syst. Res.* **2021**, *201*, 107508. [CrossRef]
9. Medina-Quesada, Á.; Montoya, O.D.; Hernández, J.C. Derivative-Free Power Flow Solution for Bipolar DC Networks with Multiple Constant Power Terminals. *Sensors* **2022**, *22*, 2914. [CrossRef]
10. Kim, J.; Cho, J.; Kim, H.; Cho, Y.; Lee, H. Power Flow Calculation Method of DC Distribution Network for Actual Power System. *KEPCO J. Electr. Power Energy* **2020**, *6*, 419–425. [CrossRef]
11. Lee, J.O.; Kim, Y.S.; Moon, S.I. Current Injection Power Flow Analysis and Optimal Generation Dispatch for Bipolar DC Microgrids. *IEEE Trans. Smart Grid* **2021**, *12*, 1918–1928. [CrossRef]
12. Chew, B.S.H.; Xu, Y.; Wu, Q. Voltage balancing for bipolar DC distribution grids: A power flow based binary integer multi-objective optimization approach. *IEEE Trans. Power Syst.* **2018**, *34*, 28–39. [CrossRef]
13. Acosta, C.; Hincapié, R.A.; Granada, M.; Escobar, A.H.; Gallego, R.A. An Efficient Three Phase Four Wire Radial Power Flow Including Neutral-Earth Effect. *J. Control. Autom. Electr. Syst.* **2013**, *24*, 690–701. [CrossRef]
14. Montoya, O.D. Notes on the Dimension of the Solution Space in Typical Electrical Engineering Optimization Problems. *Ingeniería* **2022**, *27*, e19310. [CrossRef]
15. Jesus, P.D.O.D.; Alvarez, M.; Yusta, J. Distribution power flow method based on a real quasi-symmetric matrix. *Electr. Power Syst. Res.* **2013**, *95*, 148–159. [CrossRef]
16. Albadr, M.A.; Tiun, S.; Ayob, M.; AL-Dhief, F. Genetic Algorithm Based on Natural Selection Theory for Optimization Problems. *Symmetry* **2020**, *12*, 1758. [CrossRef]
17. Abualigah, L.; Diabat, A. Advances in Sine Cosine Algorithm: A comprehensive survey. *Artif. Intell. Rev.* **2021**, *54*, 2567–2608. [CrossRef]
18. Yepes, V.; Martí, J.V.; García, J. Black Hole Algorithm for Sustainable Design of Counterfort Retaining Walls. *Sustainability* **2020**, *12*, 2767. [CrossRef]
19. Mitchell, M. Genetic algorithms: An overview. *Complexity* **1995**, *1*, 31–39. [CrossRef]
20. Attia, A.F.; Sehiemy, R.A.E.; Hasanien, H.M. Optimal power flow solution in power systems using a novel Sine-Cosine algorithm. *Int. J. Electr. Power Energy Syst.* **2018**, *99*, 331–343. [CrossRef]
21. Kumar, S.; Datta, D.; Singh, S.K. Black Hole Algorithm and Its Applications. In *Studies in Computational Intelligence*; Springer: Berlin/Heidelberg, Germany, 2014; pp. 147–170._7. [CrossRef]

22. Arenas-Acuña, C.A.; Rodriguez-Contreras, J.A.; Montoya, O.D.; Rivas-Trujillo, E. Black-Hole Optimization Applied to the Parametric Estimation in Distribution Transformers Considering Voltage and Current Measures. *Computers* **2021**, *10*, 124. [CrossRef]
23. Deeb, H.; Sarangi, A.; Mishra, D.; Sarangi, S.K. Improved Black Hole optimization algorithm for data clustering. *J. King Saud Univ. Comput. Inf. Sci.* **2020**. [CrossRef]
24. Garces, A. On the Convergence of Newton's Method in Power Flow Studies for DC Microgrids. *IEEE Trans. Power Syst.* **2018**, *33*, 5770–5777. [CrossRef]
25. Tamilselvan, V.; Jayabarathi, T.; Raghunathan, T.; Yang, X.S. Optimal capacitor placement in radial distribution systems using flower pollination algorithm. *Alex. Eng. J.* **2018**, *57*, 2775–2786. [CrossRef]